Selective and site-specific mobilization of dermal dendritic cells and Langerhans cells by Th1- and Th2-polarizing adjuvants

Debasish Sen[a], Luette Forrest[a], Thomas B. Kepler[b], Ian Parker[a,c], and Michael D. Cahalan[a,1]

[a]Department of Physiology and Biophysics and Institute for Immunology, and [c]Department of Neurobiology and Behavior, University of California, Irvine, CA 92697-4561; and [b]Center for Computational Immunology, Duke University School of Medicine, Durham, NC 27708

Edited* by Philippa Marrack, Howard Hughes Medical Institute/National Jewish Center, Denver, CO, and approved March 25, 2010 (received for review November 12, 2009)

Dendritic cells (DCs) initiate and polarize adaptive immune responses toward varying functional outcomes. By means of intravital two-photon microscopy, we report that dermal dendritic cells (DDCs) and Langerhans cells (LCs) are differentially mobilized during contact sensitization and by adjuvants such as unmethylated CpG oligonucleotide (CpG) and LPS that induce T helper type 1 (Th1) responses, or papain that induces T helper type 2 (Th2) responses. In ear pinna, contact sensitization, CpG, LPS, and papain all mobilized DDCs in three distinct phases: increased motility and dendritic probing, directed migration, and entry into lymphatic vessels. During the same treatments, the adjacent LCs in ear pinna remained immotile over a 48-hr period of observation. In contrast, footpads lacked DDCs and Th1-polarizing adjuvants selectively induced a delayed mobilization of LCs after 48 hr. Th1 polarization of CD4$^+$ T cells was independent of the immunization site, whereas ear immunization favored Th2 polarization, correlating with site-specific DC distribution and dynamics. Our results provide an initial description of peripheral DC dynamics in response to adjuvants and imply that LC mobilization enhances a Th1 response and is not sufficient to trigger a Th2 response, whereas mobilization of DDCs alone is sufficient to trigger T-cell proliferation and to polarize initial T-cell activation toward a Th2 response.

T-cell priming | two-photon microscopy | vaccine | imaging

Two-photon microscopy enables cells of the immune system to be visualized in vivo and in real time, revealing the cellular choreography of motility and interaction dynamics in lymph nodes (1). Dendritic cells (DCs) initiate the adaptive immune response by capturing antigen in the periphery; by processing and presenting endocytosed antigen as peptides bound to MHC proteins on the DC surface; and by trafficking to draining lymph nodes, where they are encountered by T cells. Endogenous DCs were first imaged in the draining lymph node following in situ labeling and maturation in the skin at an alum adjuvant injection site (2). In the draining lymph node, dermally derived DCs were observed to migrate slowly and to deploy actively probing dendrites while making frequent transient contacts with highly motile T cells (2, 3). During active immunization, DC interactions with T cells stabilize, leading to rounds of T-cell proliferation and cytokine production (3–5).

Less is known about the behavior of DC subsets and effects of adjuvants in the periphery. T-cell-mediated immune responses are characterized by specific cytokine production by activated T cells, accompanied by functional diversification of T cells. Typically, DCs respond to intracellular microbes by polarizing CD4$^+$ T cells toward a T helper type 1 (Th1) immune response, characterized by IFN-γ production by T cells. On the other hand, infection by extracellular pathogens leads to polarization of CD4$^+$ T cells toward a T helper type 2 (Th2) immune response, characterized by production of IL-4 by T cells (6). These functional specializations of activated CD4$^+$ T cells likely depend on several factors. Here, we investigate a role for adjuvant modulation of dermal dendritic cell (DDC) and Langerhans cell (LC) motility that may contribute to subsequent polarization of T-cell responses.

Vaccine adjuvants play a critical role in determining the polarization of T cells (6, 7). Adjuvants such as LPS or unmethylated CpG oligonucleoside (CpG) activate DCs via Toll-like receptors, TLR4 and TLR9, respectively; either stimulus can promote a Th1 immune response (7). Recently, it has been shown that Th2 polarization can be induced by cysteine proteases such as papain (8). Following s.c. injection in the absence of adjuvants, antigen arrives in the lymph node in two distinct waves, leading to differences in the DCs that present antigen to CD4$^+$ T cells inside draining lymph nodes (9). First, antigen draining directly into lymph nodes is presented by lymph node-resident DCs. After 24 hr, skin-draining DCs bearing processed antigen arrive and prolong the ensuing immune response. We presently have only a limited understanding of how the peripheral DC migration that contributes to the second wave of antigen presentation may shape the polarity and efficacy of the resultant immune response. Contact sensitization of skin with dibutyl phthalate and acetone (DBP-A) has also been shown to stimulate migration of DCs to draining lymph nodes (10, 11). Existing studies on selective adjuvants and contact sensitization have been limited to histology of fixed tissues at a limited number of time points (9, 12), which are static images that cannot fully represent this highly dynamic process. We therefore employed intravital two-photon microscopy to image in real time the behavior and motility of DCs in situ at sites of immunization and contact sensitization.

Here, we describe the dynamics of peripheral DC subsets mobilizing inside the tissue microenvironment at the immunization site in relation to priming of Th1 and Th2 responses by different adjuvants. Our results show that DDCs and LCs are differentially mobilized in an adjuvant- and tissue-dependent manner, implying that DC dynamics in the periphery modulate the downstream efficacy of activating and polarizing CD4$^+$ T-cell responses.

Results

Imaging DDCs, LCs, and Afferent Lymphatics Inside Ear Pinnae and Footpads. Two-photon intravital microscopy revealed LCs and DDCs in s.c. tissue of YFP-CD11c mice, together with lymphatic vessels [labeled by quantum dot conjugated anti-mouse LYVE-1 (QD-LYVE-1)] and collagen (imaged by second-harmonic generation). In

Author contributions: D.S., T.B.K., and M.D.C. designed research; D.S. and L.F. performed research; I.P. contributed new reagents/analytic tools; D.S. analyzed data; and D.S., T.B.K., I.P., and M.D.C. wrote the paper.

The authors declare no conflict of interest.

*This Direct Submission article had a prearranged editor.

[1]To whom correspondence should be addressed. E-mail: mcahalan@uci.edu.

This article contains supporting information online at www.pnas.org/cgi/content/full/0912817107/DCSupplemental.

agreement with previous histological and intravital imaging studies (10, 13), LCs inside the tissue of ear pinnae were present within 40 μm of the surface (Fig. 1A and Movie S1), exhibited numerous static dendritic processes, and were completely immotile under basal conditions. In contrast, DDCs were localized more deeply (~40–100 μm below the surface), were brighter and larger in volume compared with LCs, and had fewer but thicker dendritic processes that actively probed the environment. DDC dendrites were sometimes oriented along collagen fibers. Inside the footpad, immotile LCs were observed within 60 μm of the surface; however, surprisingly, DDCs were not observed even at depths up to 350 μm (Fig. 1*B* and Movie S2). The density of LCs inside footpads was significantly greater than the density of LCs inside ears (Fig. 1*C*). As previously observed by histological staining (11, 14), peripheral lymphatic vessels inside ear pinnae as well as footpads appeared as porous tubes with highly varying diameters that often contained branches, loops, and blind ends (Fig. 1*D* and Movie S3). Inside ear pinnae, lymphatic vessels were confined to deeper dermal tissue in closer proximity to DDCs than to LCs.

To confirm the lack of radiation-sensitive DDCs in footpads, we prepared bone marrow chimeras. In mice bearing only fluorescent DDCs but no fluorescent LCs, DDCs were observed only in ears but, again, were not found in footpads, confirming the absence of DDCs in footpads (Fig. S2 *A*, *B*, *E*, and *F*). Conversely, in chimeras having fluorescent LCs but unlabeled DDCs, LCs were observed both in ears and footpads (Fig. S2 *C*, *D*, *G*, and *H*). Thus, ear pinnae contain both deeper DDCs with motile dendrites and LCs with static dendrites, whereas footpads are predominantly populated by a high density of superficial LCs.

Mobilization of Peripheral DDCs in Ear Pinnae by Contact Sensitization in Three Phases. Under basal conditions, LCs in the ear pinnae were immotile, whereas DDCs continually scanned the environment by extension and retraction of processes, including occasional probing of dendrites into the lumen of peripheral lymphatic vessels (Fig. 2*A* and Movie S4). Although ≈20% of DDCs were motile, with average velocities between 1 and 2 μm/min, the majority were immotile although still actively probing the environment (velocities <1 μm/min). Topical application of DBP-A to ear pinnae stimulated motility of DDCs and caused them to orient and crawl toward lymphatic vessels (Fig. 2 *B*–*F* and Movie S5). We distinguished three characteristic phases during DDC mobilization, based on changes in dynamics and quantified by fitting sigmoid curves (Fig. S3): (*i*) an increase in velocity, (*ii*) orientation and homing toward peripheral lymphatic vessels, and (*iii*) entry into lymphatics (Fig. 2 *B* and *C* and Movie S5). In the first phase, DDCs began to migrate more rapidly starting 10–20 min after DBP-A treatment, acquiring velocities up to 12 μm/min (Fig. 2*C*). In phase 2, starting ~20 min after DBP-A treatment and lasting at least 90 min, motile DDCs migrated directionally toward the peripheral lymphatic vessels, characterized by sloping lines in Fig. 2*C* and sigmoid fits summarized in Fig. 2*D*. Occasionally, several DDCs were observed to follow each other along the same trajectory. In the third phase, DDCs were observed to probe the surface as well as the lumen of lymphatics for several minutes and then to enter into the lumen of peripheral lymphatic vessels. In some instances, DCs traversed along the surface of lymphatic vessels. Rarely, DCs disappeared as if swept away by lymphatic flow immediately after entry into lymphatics. More frequently, DCs continued to crawl within the

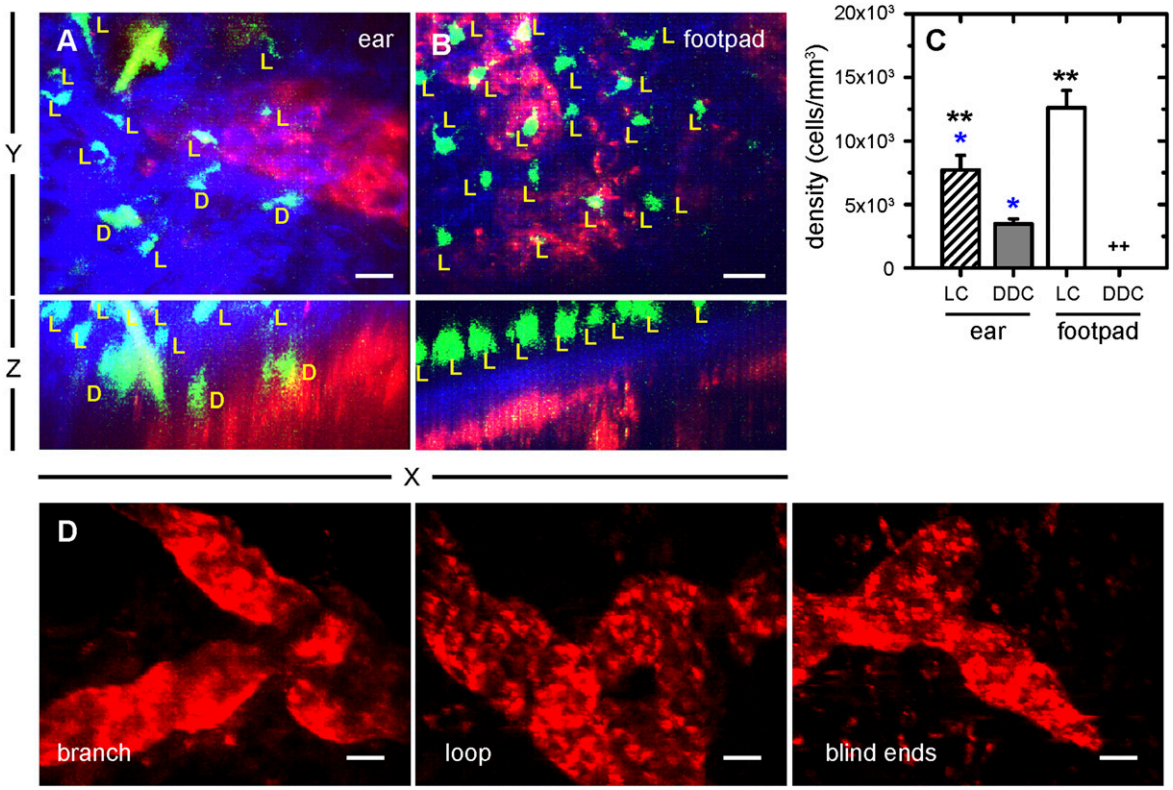

Fig. 1. CD11c⁺ LCs and DDCs differentially expressed inside ear pinnae and footpads. Two-photon images of DCs (green) inside ear pinnae and footpads of YFP-CD11c mice, lymphatic vessels (red) labeled by anti-mouse QD-LYVE-1, and collagen fibers (blue) observed by second-harmonic generation are shown. (Scale bars = 20 μm.) (*A*) DC subtypes inside ear pinnae: DDCs (labeled D) and LCs (labeled L) (Movie S1). (*B*) DCs inside footpads. Note the absence of DDCs inside the footpad; LCs are labeled as in *A*. (Movie S2). (*C*) Densities of DC subsets inside the ear and footpad measured in a standard imaging volume (200 × 150 × 100 μm³) (mean + SEM; $n = 5$ independent experiments). * and ** $P < 0.05$. Note that no DDCs were observed inside the footpad (++). (*D*) Architecture of peripheral lymphatic vessels (Movie S3).

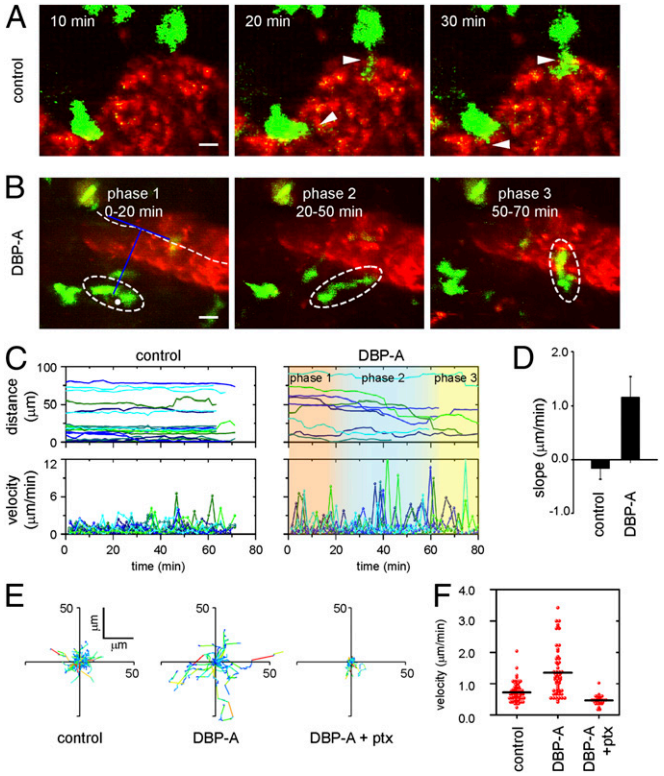

Fig. 2. Enhancement of DDC motility in ear pinnae by DBP-A. Ear pinnae of YFP-CD11c mice imaged under basal conditions (control) and after topical application of DBP-A, a contact-sensitizing agent, are shown. Lymphatic vessels (red) are labeled as in Fig. 1. (*A*) Sequential two-photon images showing probing of dendrites (arrowheads) by DDCs (green) into peripheral lymphatic vessels under basal conditions. Time elapsed after beginning imaging is shown (Movie S4). (Scale bar = 5 μm.) (*B*) Characteristic dynamic phases of an individual DDC (circled by dotted ellipse) after DBP-A application. Phase 1, mobilization illustrating the distance from the cell centroid to the center of the lymphatic vessel; phase 2, orientation and cell migration toward the lymphatic vessel; and phase 3, entry into the lymphatic vessel are shown. Time intervals after beginning imaging are shown. (Scale bar = 20 μm.) (*C*) Distances of DCs from lymphatic vessels (*Top*) and corresponding instantaneous velocities (*Bottom*) under control conditions (*Left*) and after DBP-A application (*Right*). Three different phases of DDC motility after contact sensitization are highlighted. (*D*) Average slope of tangents to sigmoid curves fit to lymphatic distance vs. time graphs of motile DCs (Fig. S3 and Movie S5). $P < 0.05$ relative to control (n = at least 10 motile cells from three independent experiments). (*E*) Normalized 45-min trajectories color-coded by instantaneous velocity, with red indicating the highest velocities and blue indicating the lowest velocities, shown for steady state (control), after DBP-A treatment, or after DBP-A plus pertussis toxin (ptx). (*F*) Velocities of individual DDCs in ear pinnae; average velocities are indicated by horizontal black bars. $P < 0.05$ for DBP-A-treated relative to control, and $P < 0.005$ relative to ptx-treated (n = at least 30 individual cells from three independent experiments) (Movie S4, Movie S5, and Movie S6).

lumen. DDC motility and probing behavior were completely abolished by pertussis toxin, indicating that a G protein-coupled receptor underlies peripheral DDC motility (Fig. 2 *E* and *F* and Movie S6). In contrast to the immediate effect in mobilizing DDCs, DBP-A treatment had no effect on LCs in either ear pinnae or footpads (Fig. S4).

Selective and Site-Specific Mobilization of DDCs and LCs by Adjuvants. Injection of CpG or LPS (Th1-inducing adjuvants) or of papain (Th2-inducing adjuvant) significantly enhanced DDC motility in ear pinnae. Similar to contact sensitization, each adjuvant induced the same three phases of DDC mobilization (Fig. S5 and Movie S7, Movie S8, Movie S9, and Movie S10). Over 25% of DDCs exhibited average velocities >2 μm/min, with peak velocities >12 μm/min (Fig. S5*A*). Similar to DDC behavior observed during contact sensitization by DBP-A, on reaching the lymphatic vessels, DDCs actively probed the lymphatic lumen by extension of dendrites (Fig. 3*A*) or traveled along the surface of lymphatic vessels on entry before being swept away. Increased DDC motility in the pinnae was sustained for at least 48 hr after immunization with Th1 as well as Th2 adjuvants (Fig. 3 *B* and *C*). Mobilized DCs exhibited similar changes in velocities, and similar rates of directional movement toward lymphatic vessels (phase 2) were measured for each adjuvant (Fig. 3*D*).

LCs were entirely immotile before and immediately following adjuvant injection. However, >15% of LCs inside footpads acquired motility ~48 hr after CpG or LPS injection (Fig. 4 *A* and *B* and Movie S11 and Movie S12), exhibiting velocities >1 μm/min. Among LCs that remained immotile 48 hr after CpG or LPS stimulation, >25% exhibited increased probing of dendritic processes compared with basal conditions. LC motility and dendritic probing inside footpads were unaffected by papain (Movie S13). In

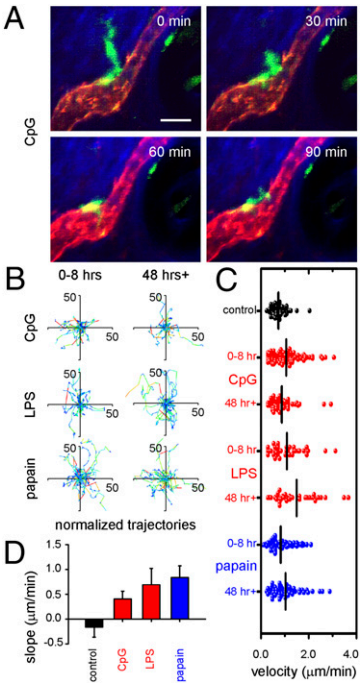

Fig. 3. Modulation of DDC motility in ear pinnae by CpG, LPS, and papain. DDCs (green), collagen (blue, second harmonic), and lymphatic vessels (red) are imaged after s.c. injection of CpG, LPS, or papain. (*A*) Sequential frames showing an individual DDC scanning the surface of a lymphatic vessel and probing into the lymphatic lumen after stimulation with CpG. Time elapsed after beginning imaging is shown (Movie S7). (Scale bar = 20 μm.) (*B*) Normalized trajectories of DDCs in ear pinnae within the first 8 hr after stimulation (*Left*) and 48 hr or more after stimulation (*Right*) with CpG, LPS, or papain, as indicated. All trajectories begin at the origin and indicate the path traced out by individual DDCs in 45 min. As in Fig. 3*E*, red indicates the highest velocities and blue indicates lower velocities. (*C*) Distribution of average velocities of DDCs inside ears under the indicated stimuli. Control (black), Th1-inducing (red), and Th2-inducing (blue) adjuvants are as labeled. Average velocities are indicated by vertical black bars; $P < 0.05$ for CpG-, LPS-, and papain-treated at 0–8 hr and after 48 hr relative to control, but $P > 0.05$ compared with each other (n = at least 30 cells from three independent experiments). (*D*) Slopes indicating rates of DC directional migration, determined by fitting a sigmoid function to the normalized distance between individual motile DCs and lymphatic vessels after CpG, LPS, or papain application. $P < 0.005$ for CpG-, LPS-, and papain-treated relative to control, but $P > 0.05$ compared with each other [n = at least 10 motile DCs (velocity >1.0 μm/min) from three independent experiments] (Figs. S3 and S4 and Movie S8, Movie S9, and Movie S10).

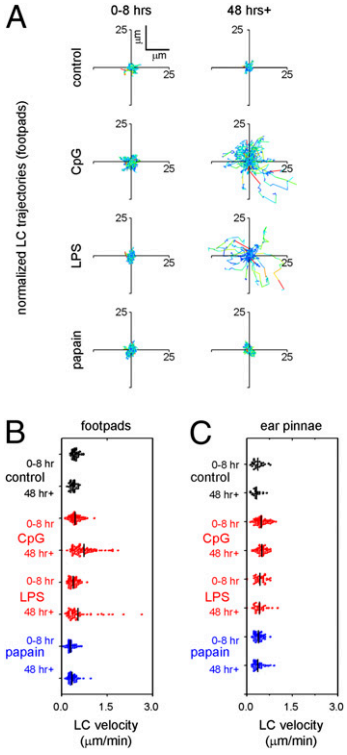

Fig. 4. CpG and LPS but not papain mobilize LCs inside footpad after ~48 hr. LCs in footpads were imaged under basal conditions or after s.c. injection of CpG, LPS, or papain. (*A*) Normalized 45-min trajectories of LCs inside footpads within the first 8 hr (*Left*) and 48 hr or more (*Right*) after stimulation with CpG, LPS, or papain as indicated. Colors indicate velocities as in Figs. 2*E* and 3*B*. (*B*) Distribution of average velocities of LCs inside footpads under the indicated stimuli. Average velocities are indicated by vertical black bars for each condition. Control (black), Th1-inducing (red), and Th2-inducing (blue) adjuvants (Movie S11, Movie S12, and Movie S13). $P < 0.05$ for CpG- and LPS-treated at 48 hr compared with P values of CpG- and LPS-treated at 0–8 hr, respectively, and $P < 0.05$ compared with control (n = at least 60 cells from three independent experiments). (*C*) Corresponding average velocities of LCs inside ears after the indicated stimuli. $P > 0.05$ for each adjuvant compared with control and each other (n = at least 30 cells from three independent experiments).

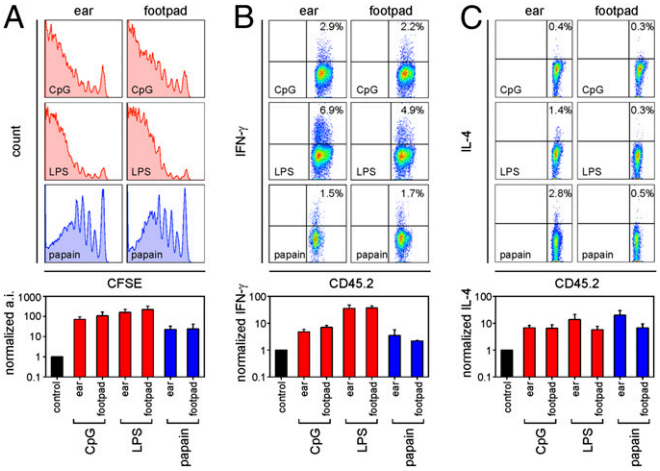

Fig. 5. Proliferation and cytokine production by cognate CD4$^+$ T cells after ear and footpad immunization. Th1 adjuvants (red) and Th2 adjuvants (blue) are shown. P values (n = 3 independent experiments) are represented as $P_{x,\,y}$, where x and y are either adjuvants or immunization sites that are being compared. Bar graphs of proliferation, IFN-γ production, and IL-4 production are on logarithmic scales and normalized to unimmunized controls (control). (*A*) Proliferation in CD45.1$^+$ BL/6 mice of OT-II T cells under the immunization conditions indicated, measured by carboxyfluorescein succinimidylester dilution after 5 days (*Left*, ear pinna; *Right*, footpad). The activation index (a.i.) for T-cell proliferation is indicated for each immunization condition and site. $P_{papain,\ LPS} < 0.005$, $P_{papain,\ CpG} < 0.005$. (*B*) Production of intracellular IFN-γ in CD4$^+$ T cells under the conditions indicated inside the plots. (*Lower*) Normalized levels of IFN-γ are shown. $P_{CpG,\ LPS} < 0.05$, $P_{papain,\ LPS} < 0.01$, and $P_{papain,\ CpG} < 0.01$. (*C*) Corresponding measures of IL-4 production for each immunization condition and site. $P_{footpad,\ ear} < 0.05$ for LPS and papain, $P_{papain,\ LPS} < 0.05$, and $P_{papain,\ CpG} < 0.05$.

contrast to pronounced mobilization of footpad LCs by CpG or LPS, no appreciable changes in LC motility were observed within ear pinnae following s.c. injection of CpG, LPS, or papain (Fig. 4*C*). Thus, in contrast to DDC mobilization, LC mobilization is a slower process that is both adjuvant- and site-specific.

Adjuvant and Tissue Dependence of CD4$^+$ T-Cell Priming. We next investigated whether the absence of DDCs in footpads and differential mobilization of LCs by adjuvants correspond to CD4$^+$ T-cell priming and polarization (Fig. 5). CpG and LPS facilitated T-cell proliferation to a greater extent than papain and to an equal extent in footpad or ear (Fig. 5*A*). To isolate the contribution of LCs to T-cell priming, we employed Diphtheria toxin receptor (DTR)→B6 mouse chimeras to deplete CD11c-expressing DDCs and lymph node-resident DCs selectively. In these mice, treatment with diphtheria toxin depleted DTR-CD11c$^+$ DCs by >95%. T-cell proliferation was significantly reduced following immunization in ears but to a lesser extent in footpads, which still contained predominantly LCs (Fig. S6). Together, these results indicate that mobilized DDCs or lymph node-resident DCs can trigger initial T-cell proliferation, whereas delayed mobilization of LCs alone may also contribute to enhancing T-cell proliferation in draining lymph nodes. Second, and correlating with mobilization of LCs, IFN-γ production (indicating Th1 polarization) was enhanced in an adjuvant-dependent (LPS > CpG >> papain) and site-independent manner (Fig. 5*B*). Thus, conditions that favor LC mobilization in addition to DDC mobilization (Figs. 3 and 4) are correlated with a robust Th1 response. In contrast, the efficacy of Th2 polarization was both adjuvant- and site-dependent (Fig. 5*C*). The adjuvant dependence of IL-4 production (papain >> LPS ≈ CpG) parallels selective mobilization of DDCs without LCs. Moreover, IL-4 was less efficiently induced following footpad immunization, where only LCs but no DDCs are present. In summary, conditions favoring LC mobilization in addition to DDC mobilization (Figs. 3 and 4) are correlated with a robust Th1 response, whereas DDC mobilization in the absence of LC mobilization promotes a Th2 response.

Discussion

Our results, summarized in Table S1, show that mobilization of peripheral DC subsets is both adjuvant- and tissue-dependent and that the patterns of DC mobilization correlate with distinct outcomes of T-cell priming. Differential DC dynamics are likely to play a role in determining responses to adjuvants that induce distinct Th1 or Th2 immune polarization, but peripheral DC behavior had not previously been visualized during this process. Inside mouse ear pinnae, Th1 or Th2 adjuvants and contact sensitization induced robust and immediate changes in DDC probing, velocities, and lymphatic homing behavior. Neighboring LCs, however, remained immotile even after 2 days. In contrast, inside footpads that are marked by a surprising lack of DDCs, LCs were not immediately affected by adjuvant treatment; however, after 2 days, they acquired motility following injection of CpG or LPS (Th1-polarizing adjuvants) but not following contact sensitization (DBP-A) or injection of papain (Th2-polarizing adjuvant). This

is a demonstration of a direct correlation between LC mobilization and Th1 enhancement accompanied by Th2 inhibition. Moreover, we show that promotion of a Th2 response may occur downstream of DDC mobilization alone, provided that LCs are not mobilized. It will be interesting to investigate whether other leukocytes or intracellular signaling pathways participate in mobilized DC subset-mediated T-cell polarization.

The immediate effects of adjuvant stimuli on DDC migration and the slower induction of LC migration at the sites of adjuvant injection are consistent with the findings of previous studies showing that the arrival of LCs inside lymph nodes is delayed by 2–3 days, whereas DDCs arrive in lymph nodes within 24 hr of adjuvant injection (3, 9, 10, 15, 16). Mobilization of DDCs by the four agents tested occurred in three distinct phases: increased dendritic probing and velocity, orientation and directed migration toward lymphatic vessels, and probing and entry into the lymphatic vessels. Even phase 1 (increased motility and dendritic probing) was blocked by local pertussis-toxin treatment, indicating that a G protein receptor underlies the earliest phases of peripheral DDC migration and accounting for pertussis-toxin inhibition of DDC migration to lymph nodes reported previously (9, 12). At minimal observed lymph flow rates of 200 μm/min (17), DCs swept away by lymph flow would arrive at the draining lymph node within 2 hr. Our results show that DCs reach peripheral lymphatic vessels within an hour of stimulus but, thereafter, either crawl along lymphatic vessels with velocities much lower than lymphatic flow or actively probe dendrites into lymphatic lumen for hours. Therefore, dynamic interactions of DCs with peripheral lymphatic vessels during phase 3 of lymphatic homing, before being washed away by lymphatic flow, is likely the rate-limiting step for DC arrival to draining lymph nodes.

We further show that Th1 adjuvants, which induced immediate and robust mobilization of DDCs in ear pinnae and delayed mobilization of LCs in footpads, also induced efficient $CD4^+$ T-cell proliferation as well as robust IFN-γ production independent of the site of immunization. Inside the node during the first day of immunization, three phases of T-cell–DC interaction have been described for both $CD4^+$ and $CD8^+$ T cells: (*i*) initial transient interactions resulting in serial contacts with multiple DCs, (*ii*) stable T-cell–DC contacts lasting for hours, and (*iii*) swarming T cells that disengage from DCs and again contact additional DCs serially (1, 3, 5). All three phases in the lymph node are mediated by the more rapidly arriving DDCs. These T-cell–DC interactions, as well as antigen presentation by resident DCs (9), can promote robust T-cell proliferation. Late arriving antigen-bearing LCs, however, may be required to enhance T-cell priming toward a full-blown Th1 response. Consistent with this interpretation, it was previously shown that a second round of s.c.-injected antigen-bearing DCs arriving inside lymph nodes 48 hr or more following the initial T-cell activation phases led to enhanced IFN-γ production (18). In that study, the DCs were pulsed with antigen in vitro and reinjected following the initial phases of T-cell activation induced by a first round of DCs. Our results with a single immunization using Th1-promoting adjuvants suggest that the more slowly migrating LCs selectively induced by CpG or LPS supply the second wave of antigen to the node that enhances a Th1 response. Our results, using local administration of LPS, are in apparent conflict with those of a previous report showing inhibition of DDC motility by systemic injection of LPS (13). Differential effects on motility of peripheral DCs may result from systemic vs. local administration.

In contrast, a Th2-inducing adjuvant that affected DDC motility alone but had no effect on LC motility in either the ear pinna or footpad induced less efficient T-cell proliferation compared with Th1 adjuvants. Moreover, IL-4 production was strongly enhanced on ear immunization with Th2 adjuvants but not in footpads that lacked DDCs. These results suggest that although both DDC and LC motility in the periphery underlies efficient Th1 immune responses, mobilization of DDCs alone, without LC mobilization, may bring about Th2 immune responses. Recently, basophils in lymph nodes have also been implicated in Th2 responses as IL-4-inducing antigen-presenting cells (8, 19–21). However, basophils are not normally present in peripheral tissue (8, 20) and can only be observed in draining lymph nodes after 2–3 days (8). Thus, migratory DDCs are necessary to convey antigen and adjuvant information to the lymph node and to subsequently engage basophils in the lymph node, in addition to activating $CD4^+$ T cells to initiate Th2 responses. Differential effects of Th1 or Th2 adjuvant on DDC or LC mobilization can therefore determine the subsequent polarization of an immune response. The roles of cutaneous LCs in inducing T-cell-mediated immune responses remain unclear. Although Igyarto et al. (22) demonstrated that LCs can possibly downmodulate T-cell-mediated contact hypersensitivity responses on abdominal contact sensitization, Wang et al. (23) have shown that LCs can enhance or suppress contact sensitization under varying immunization conditions, with down-regulation of T-cell-mediated contact sensitization being observed only on abdominal but not ear immunization. Our data suggest that the differential distribution of LCs and DDCs at different immunization sites also may play a role in determining the efficacy of Th polarization on s.c. immunization in an antigen-specific context.

DC subsets are differentially distributed in the ear pinnae and footpads. Notably, DDCs are lacking in footpads, which naturally come into direct contact with the ground, and may therefore encounter significantly more pathogens or parasites compared with ear pinnae. We suggest that the footpad is designed for detection and response to intracellular parasites that induce Th1 responses via LCs and that the absence of sensitive DDCs may ensure that the footpad is not chronically inflamed. Our observations show that tissue-specific differences in peripheral DC dynamics correlate with the efficiency of immune polarization and highlight the importance of the site of immunization for vaccine efficiency.

Materials and Methods

Mice. Mice expressing enhanced YFP on a CD11c promoter (YFP-CD11c mice) (24) were a kind gift of M. Nussenzweig (The Rockefeller University, New York, NY) and were backcrossed to B6 for 10 generations. C57BL/6, congenic CD45.1 BL/6 (no. 2014), T-cell receptor transgenic ova-IA^b-specific OT-II mice (no. 4194), and DTR-CD11c BL/6 (no. 4509) mice were purchased from the Jackson Laboratory. Mice were maintained in a pathogen-free facility, and all experiments were performed in accordance with a protocol approved by the Institutional Animal Care and Use Committee of the University of California, Irvine.

Intravital Imaging. Ears or footpads of anesthetized mice were mounted on the temperature-controlled stages (Fig. S1) and immersed in 20% vol/vol glycerol in PBS. No depilating agents were used because we observed significant changes in DDC motility induced by using topical depilatory reagents. Peripheral lymphatic vessels were labeled by s.c. injection of 5 μL of PBS containing ~1 μg of QD-LYVE-1 in the presence or absence of adjuvants. In separate experiments, 5 μL of PBS containing 25 μg of either CpG, LPS, or papain was s.c. injected into ears or footpads. For contact sensitization, 50 μL of a 1:1 mixture of dibutyl phthalate and acetone (DBP-A) was topically applied to ear pinnae or footpads before imaging. Images were acquired with a custom-built, video-rate, two-photon microscope as previously described (16, 25). Unless otherwise mentioned, images corresponding to each time point represented X × Y × Z = 200- × 150- × 100-μm^3 sections. Image analyses and generation of time-lapse movies were performed using MetaMorph (Molecular Devices Inc.), Imaris (Bitplane Inc.), Photoshop CS4 (Adobe Systems Inc.), Premiere CS4 (Adobe Systems Inc.), and custom software (described in *SI Text*).

Bone Marrow Reconstitution. To distinguish radiation-resistant LCs, radiation-sensitive DDCs, and lymph node-resident DCs, bone marrow chimeras were generated as previously described (26). Briefly, host mice were lethally irradiated with two doses of 550 cGy separated by 3 hr, followed by reconstitution for at least 8 weeks with 5×10^6 freshly isolated bone marrow

cells from donor mice. Donor–recipient pairs used for generating chimeras are as follows:

Donor: congenic CD45.1 BL/6, Recipient: YFP-CD11c (B6→YFP)
Donor: YFP-CD11c, Recipient: congenic CD45.1 BL/6 (YFP→B6)
Donor: DTR-CD11c, Recipient: congenic CD45.1 BL/6 (DTR→B6)

Single-cell suspensions obtained from tissues from ear pinnae and footpads of bone marrow-reconstituted as well as WT mice were assessed for phenotypes of LCs and DDCs.

Activation of CD4$^+$ T Cells and Measurement of Cytokines. Enriched ovalbumin-specific CD4$^+$ T cells from OT-II mice were adoptively transferred into recipient mice, followed by s.c. immunization of ears or footpads of these mice with 50 μg of ovalbumin included in 5 μL of PBS containing 25 μg of CpG, 25 μg of LPS, 25 μg of papain, or PBS alone. Lymphocytes were recovered from lymph nodes and spleens 5 days later and examined for proliferation, IFN-γ production, and IL-4 production by ovalbumin-specific T cells. Proliferation was quantified in terms of activation indices, as previously described (16). Cytokine levels and activation indices were normalized to those of unstimulated controls.

ACKNOWLEDGMENTS. We thank Kym Garrod, Bali Pulendran, and Tang Hua for helpful comments and advice and M. Nussenzweig for the enhanced YFP-CD11c mice. This research was supported by National Institutes of Health Grants GM-41514 (to M.D.C.) and GM-48071 (to I.P.) and by Biodefense Subcontract N01-AI-50019 (to M.D.C.).

1. Cahalan MD, Parker I (2008) Choreography of cell motility and interaction dynamics imaged by two-photon microscopy in lymphoid organs. *Annu Rev Immunol* 26: 585–626.
2. Miller MJ, Hejazi AS, Wei SH, Cahalan MD, Parker I (2004) T cell repertoire scanning is promoted by dynamic dendritic cell behavior and random T cell motility in the lymph node. *Proc Natl Acad Sci USA* 101:998–1003.
3. Miller MJ, Safrina O, Parker I, Cahalan MD (2004) Imaging the single cell dynamics of CD4+ T cell activation by dendritic cells in lymph nodes. *J Exp Med* 200:847–856.
4. Bousso P, Robey E (2003) Dynamics of CD8+ T cell priming by dendritic cells in intact lymph nodes. *Nat Immunol* 4:579–585.
5. Mempel TR, Henrickson SE, Von Andrian UH (2004) T-cell priming by dendritic cells in lymph nodes occurs in three distinct phases. *Nature* 427:154–159.
6. Agrawal S, et al. (2003) Cutting edge: Different Toll-like receptor agonists instruct dendritic cells to induce distinct Th responses via differential modulation of extracellular signal-regulated kinase-mitogen-activated protein kinase and c-Fos. *J Immunol* 171:4984–4989.
7. Pulendran B, Ahmed R (2006) Translating innate immunity into immunological memory: Implications for vaccine development. *Cell* 124:849–863.
8. Sokol CL, Barton GM, Farr AG, Medzhitov R (2008) A mechanism for the initiation of allergen-induced T helper type 2 responses. *Nat Immunol* 9:310–318.
9. Itano AA, et al. (2003) Distinct dendritic cell populations sequentially present antigen to CD4 T cells and stimulate different aspects of cell-mediated immunity. *Immunity* 19:47–57.
10. Kissenpfennig A, et al. (2005) Dynamics and function of Langerhans cells in vivo: Dermal dendritic cells colonize lymph node areas distinct from slower migrating Langerhans cells. *Immunity* 22:643–654.
11. Randolph GJ, Angeli V, Swartz MA (2005) Dendritic-cell trafficking to lymph nodes through lymphatic vessels. *Nat Rev Immunol* 5:617–628.
12. Lämmermann T, et al. (2008) Rapid leukocyte migration by integrin-independent flowing and squeezing. *Nature* 453:51–55.
13. Ng LG, et al. (2008) Migratory dermal dendritic cells act as rapid sensors of protozoan parasites. *PLoS Pathog* 4:e1000222.
14. Roediger B, Ng LG, Smith AL, Fazekas de St Groth B, Weninger W (2008) Visualizing dendritic cell migration within the skin. *Histochem Cell Biol* 130:1131–1146.
15. Shklovskaya E, Roediger B, Fazekas de St Groth B (2008) Epidermal and dermal dendritic cells display differential activation and migratory behavior while sharing the ability to stimulate CD4+ T cell proliferation in vivo. *J Immunol* 181:418–430.
16. Sen D, Deerinck TJ, Ellisman MH, Parker I, Cahalan MD (2008) Quantum dots for tracking dendritic cells and priming an immune response in vitro and in vivo. *PLoS One* 3:e3290.
17. Swartz MA, Berk DA, Jain RK (1996) Transport in lymphatic capillaries. I. Macroscopic measurements using residence time distribution theory. *Am J Physiol* 270:H324–H329.
18. Celli S, Garcia Z, Bousso P (2005) CD4 T cells integrate signals delivered during successive DC encounters in vivo. *J Exp Med* 202:1271–1278.
19. Perrigoue JG, et al. (2009) MHC class II-dependent basophil-CD4+ T cell interactions promote T(H)2 cytokine-dependent immunity. *Nat Immunol* 10:697–705.
20. Sokol CL, et al. (2009) Basophils function as antigen-presenting cells for an allergen-induced T helper type 2 response. *Nat Immunol* 10:713–720.
21. Yoshimoto T, et al. (2009) Basophils contribute to T(H)2-IgE responses in vivo via IL-4 production and presentation of peptide-MHC class II complexes to CD4+ T cells. *Nat Immunol* 10:706–712.
22. Igyarto BZ, et al. (2009) Langerhans cells suppress contact hypersensitivity responses via cognate CD4 interaction and langerhans cell-derived IL-10. *J Immunol* 183: 5085–5093.
23. Wang L, et al. (2008) Langerin expressing cells promote skin immune responses under defined conditions. *J Immunol* 180:4722–4727.
24. Lindquist RL, et al. (2004) Visualizing dendritic cell networks in vivo. *Nat Immunol* 5: 1243–1250.
25. Nguyen QT, Callamaras N, Hsieh C, Parker I (2001) Construction of a two-photon microscope for video-rate Ca(2+) imaging. *Cell Calcium* 30:383–393.
26. Merad M, et al. (2002) Langerhans cells renew in the skin throughout life under steady-state conditions. *Nat Immunol* 3:1135–1141.